Turbulent Diffusion in the Core of a Pipe with Uniform Transverse Flow at the Walls

S. K. SUNEJA, R. H. SHEA and D. T. WASAN

Department of Chemical Engineering
Illinois Institute of Technology, Chicago, Illinois 60616

An analysis of point source turbulent diffusion of a gaseous tracer in the core of a circular straight porous pipe with uniform transverse flow at the walls is presented. Time averaged concentration distributions were measured at four distances downstream from a point source located at the axis of a fully developed turbulent flow of air in a 6-in. pipe. Experiments were run at average velocities between 4.36 and 23.0 ft./sec. (corresponding to Reynolds numbers 12,000 to 66,000) with injection velocities ranging from 0 to 0.170 ft./sec. and suction velocities from 0 to 0.048 ft./sec. The highest injection rate corresponded to 58% by volume of the main stream. Good agreement is obtained between the experimental and the calculated concentration profiles.

The present study shows that the plume width of the dispersing tracer is considerably affected by the transverse flow. It also shows that the eddy diffusivity in the pipe core and the radial mass flux increase with fluid injection and decrease with suction through the pipe walls. Also, for increasing values of aspect ratio, they increase in the case of injection and decrease in the case of fluid suction.

The diffusion of a substance from a point source into a turbulent field has received much attention from investigators in various engineering disciplines (*1* to *26*). An understanding of this process is important with respect to controlling the emission of smoke and other pollutants into the atmosphere and the flow of wastes into rivers and streams. In addition, it provides a basis for evaluating eddy diffusivities (*7, 10, 17, 26*) and other properties of turbulence in such unit operations as heat transfer, extraction, mixing, absorption, and humidification.

Investigations of point source diffusion in ducted streams have involved statistical methods (*9, 11, 24, 25*) as well as experiments with various gases (*2, 6, 14, 17, 26*), liquids (*7, 12, 13*), and mixed systems (*3* to *5, 8, 10, 18, 20, 22,* 23) in flow configurations ranging from rectangular ducts (*12, 18*) to large circular pipes (*2, 14*) and at Reynolds numbers from about 10,000 (*6*) up to 500,000 (*2, 14*). Although these and similar studies have examined the effects of numerous factors, including concentration (*13, 17*), temperature (*1, 15, 19*), velocity (*2, 18, 26*), and intensity of turbulence (*6, 7*), there has been no previous work on the problem of transverse flow.

Transverse flow, induced by either injection or suction at the duct wall can significantly influence the velocity and concentration profiles of diffusing substances. Consequently, it has important implications in the design of porous-walled transpiration reactors and in other applications requiring high flux mass transfer. As part of a general study of point source diffusion (*21*), we have therefore developed expressions to describe the effects of transverse flow on the diffusion of tracer gases in a turbulent field. The expressions have been tested in experiments on the diffusion of helium into air within a porous circular pipe while air was either injected or withdrawn through the pipe walls.

Correspondence concerning this paper should be addressed to D. T. Wasan. S. K. Suneja is with Amoco Chemicals Corp., Naperville, Illinois and R. H. Shea is with Mobil Oil Company, Chicago, Illinois.

THEORETICAL ANALYSIS

The system of interest is shown in Figure 1, where the radial and longitudinal coordinates are also indicated. To describe the effects of transverse flow, expressions for three quantities are needed: the concentration of the tracer, the eddy diffusivity for material transport, and the radial mass flux. The following assumptions are made:

1. The fluids are incompressible and isothermal.
2. The main stream turbulent flow is fully developed at the entrance to the porous pipe.
3. Fluids flowing in the axial direction and through the porous walls have similar physical properties.
4. The wall flow is uniform throughout the length of the porous section; that is, the radial velocity at the wall does not vary with the longitudinal distance.

Concentration of Tracer

The material balance for the diffusing tracer—designated as A—over a differential element yields the equation:

$$u\frac{\partial C_A}{\partial x} + v\frac{\partial C_A}{\partial r} = \frac{\epsilon}{r}\frac{\partial}{\partial r}\left(r\frac{\partial C_A}{\partial r}\right) + \frac{\partial C_A}{\partial r}\frac{\partial \epsilon}{\partial r} \quad (1)$$

where the molecular diffusion is neglected compared to convective diffusion in the axial direction. Also the overall continuity equation may be expressed (*21*) as:

$$u = u_{av}u^* = (u_{avi} - 4\,v_w x/D)u^* \quad (2)$$

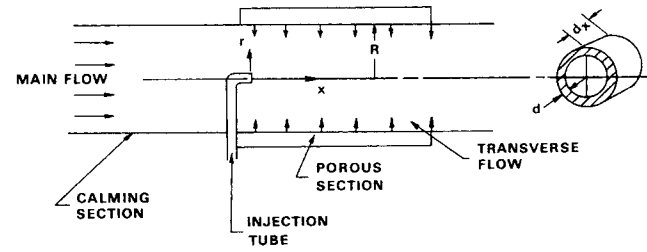

Fig. 1. Schematic diagram of the system analyzed

where u^* is the dimensionless velocity at a point and varies with radial distance only. The boundary conditions are taken as:

$$C_A = 0 \quad \text{as } r \to \infty \tag{3}$$

$$\partial C_A/\partial r = 0 \text{ at } r = 0; \quad C_A = 0 \text{ at } x = 0, \quad r > b \tag{4}$$

where Equation (3) implies that the diffusing material does not reach the tube walls, and therefore treats the fluid as infinite in the radial direction. For no transverse flow (that is, $v = 0$) the solution is (*1, 10*):

$$C_A(x, r) = \frac{Q}{4\pi x \epsilon_{c0}} \exp\left(-\frac{r^2 u_{c0}}{4 x \epsilon_{c0}}\right) \tag{5}$$

We therefore assume that the solution to Equation (1) with transverse flow (that is, $v \neq 0$) is of the analogous form:

$$C_A(x, r) = \frac{Q}{\pi u_c m} \exp(-r^2/m) \tag{6}$$

where m is a function of x, and Q is the volumetric rate of injection of tracer material. For isokinetic injection, $Q = \Pi b^2 u_{ci}$. Substituting the expressions for $\partial C_A/\partial r$ and $\partial C_A/\partial x$ from Equation (6) into Equation (1) and using the overall continuity Equation (2), the following two equations result.

$$\frac{2 v_w}{R u_{av}} - \frac{1}{m}\frac{dm}{dx} + \frac{4\epsilon}{u m} = 0 \tag{7}$$

and

$$-\frac{r^2}{m}\frac{dm}{dx} + \left(\frac{\partial \epsilon}{\partial r} - v\right)\frac{2r}{u} + \frac{4r^2}{m}\frac{\epsilon}{u} = 0 \tag{8}$$

where the terms in Equation (7) are functions of x alone, while those in Equation (8) are functions of both x and r, provided the term ϵ/u does not vary with radial position. As indicated by Schlinger and Sage (*17*), this is a reasonable assumption for the core region of the pipe. This assumption permits the relationship

$$\frac{\epsilon}{u} = \frac{\epsilon_c}{u_c} \tag{9}$$

where ϵ_c is the eddy diffusivity at the pipe axis.

Substituting Equation (9) into Equation (7) gives

$$\frac{dm}{dx} = \frac{2 v_w}{R u_{av}} m + 4\frac{\epsilon_c}{u_c} \tag{10}$$

whose solution requires a prior knowledge of the functional form of ϵ_c, which varies with the longitudinal distance. In analogy to the functional form for ϵ_{c0}, we assume that ϵ_c is of the form pu_c^a where p and 'a' are not functions of x and u_c varies with x. Substituting pu_c^a for ϵ_c and $u_{av}u_c^*$ for u_c [from Equation (2)] in Equation (10) gives

$$\frac{dm}{dx} - \frac{2 v_w}{R u_{av}} m = 4 p u_c^{a-1} u_{av}^{a-1} \tag{11}$$

Equation (11) is a first-order differential equation with variable coefficients, and its solution is

$$m = \frac{4 p u_c^{a-1} u_{avi}^a}{(a+1)(-2 v_w/R)}\left[\left(1 - 4\phi\frac{x}{D}\right)^a - \frac{1}{(1 - 4\phi x/D)}\right] + \frac{b^2}{(1 - 4\phi x/D)} \tag{12}$$

In this solution, the parameters p and a are yet to be determined. However, p can be determined on the basis that this solution must reduce to Equation (5) for the case of $v_w = 0$. This gives

$$p = \epsilon_{c0}/u_{c0}^a \tag{13}$$

where ϵ_{c0} is the eddy diffusivity at the pipe axis in the absence of transverse flow. We now assume that over a distance of a few pipe diameters the turbulence energy per unit mass in the core is unaffected by transverse flow (since reaction takes time) so that the parameter a in the presence of transverse flow is the same as in the absence of it, that is, 0.875. This is borne out by the agreement of the theory with the data as discussed later in this paper. On this basis Equation (12) becomes

$$m = \frac{-0.533 D}{\phi}\frac{\epsilon_{c0}}{u_{c0}}\left[(1 - 4\phi x/D)^{0.875} - \frac{1}{(1 - 4\phi x/D)}\right] + \frac{b^2}{(1 - 4\phi x/D)} \tag{14}$$

Substitution of Equation (14) into Equation (6) yields the following solution:

$$\frac{C_A(x, r)}{C_{Ac}} = \exp\left[\frac{-r^2(1 - 4\phi x/D)}{\frac{-0.533 D}{\phi}\frac{\epsilon_{c0}}{u_{c0}}\{(1 - 4\phi x/D)^{1.875} - 1\} + b^2}\right] \tag{15}$$

where

$$C_{Ac} = \frac{Q(1 - 4\phi x/D)}{\pi u_c\left[b^2 - 0.533\frac{D}{\phi}\frac{\epsilon_{c0}}{u_{c0}}\{(1 - 4\phi x/D)^{1.875} - 1\}\right]} \tag{16}$$

Here b^2 represents the correction due to the finite size of the injection tube. Because the internal diameter of the injection tube is generally quite small, b^2 is often much less than $\frac{0.533 D}{\phi}\frac{\epsilon_{c0}}{u_{c0}}\left[\left(1 - 4\phi\frac{x}{D}\right)^{1.875} - 1\right]$ and so can be neglected.

To compute the concentration profiles C_A/C_{AC} from Equation (15), one needs to know the value of ϵ_{c0}, which is a function of the entrance Reynolds' number and is obtained from the data for no transverse flow (*27*). Our data (*21*) indicates the following relationship for entrance Reynolds number up to 80,000:

$$\epsilon_{\text{core, 0}} \approx \epsilon_{c0} = 0.005\frac{\mu}{\rho} Re_{IN}^{0.875} \tag{17}$$

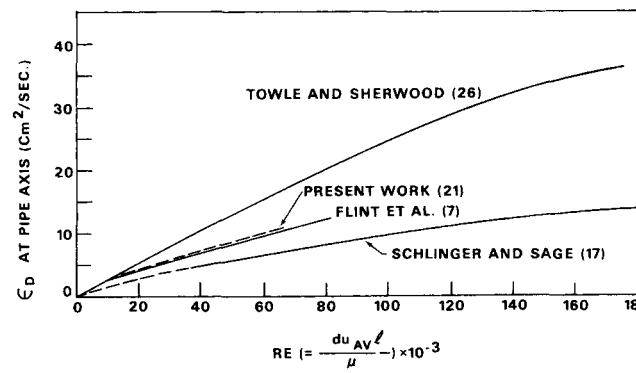

Fig. 2. Eddy diffusivity at the pipe axis versus Reynolds number for no transverse flow.

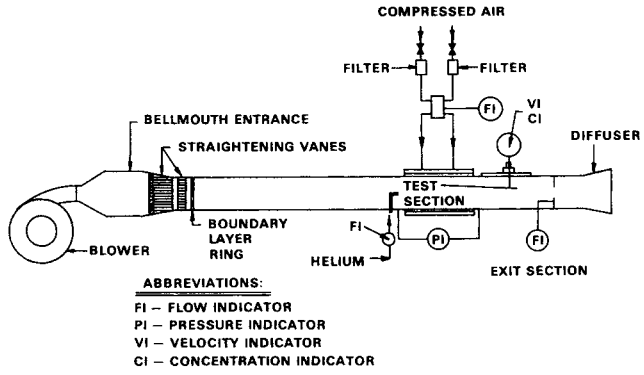

Fig. 3. A schematic view of the experimental equipment.

As shown in Figure 2, this correlation agrees closely with the data reported by Flint et al (7).

Eddy Diffusivity for Material Transport

For calculating eddy diffusivity, Equation (1) can be rearranged in the following form:

$$\epsilon(x,r) = \frac{1}{r\dfrac{\partial C_A}{\partial r}}\left[\int_0^r r\,u\frac{\partial C_A}{\partial x}\,dr + \int_0^r r\,v\frac{\partial C_A}{\partial r}\,dr\right] \tag{18}$$

The system considered here is such that the radial concentration gradients (that is, $\partial C_A/\partial r$) go through large variations in radial direction, so that the values calculated from Equation (18) involve large errors (due to the inaccuracies in the value of $\partial C_A/\partial r$), away from the pipe axis. However, consistent with the assumption made earlier in this analysis, eddy diffusivity in the core region can be considered essentially constant and be taken same as at the pipe axis. So taking the limit of Equation (18) for $r \to 0$ and inserting the expressions for $\partial C_A/\partial x$ and $\partial^2 C_A/\partial r^2$ from Equation (15) and for ϵ_{c0} from Equation (17) gives

$$\epsilon_c(x) \approx \epsilon_{\text{core}}(x) = \frac{u_c}{2}\left[\frac{\partial C_A/\partial x}{\partial^2 C_A/\partial r^2}\right]_{r=0} = \frac{u_c}{4}\frac{dm}{dx} - \frac{u_c}{u_{av}}\frac{v_w}{D}m \tag{19}$$

where m is given by Equation (14) and dm/dx is given by the following expression:

$$\frac{dm}{dx} = \frac{2.132}{(1-4\phi x/D)^2}\frac{\epsilon_{c0}}{u_{c0}}\left[0.875(1-4\phi x/D)^{1.875}+1\right] \tag{20}$$

Using Equation (19), one can compute longitudinal profiles for the eddy diffusivity in the presence of transverse flow for any desired values of the entrance Reynolds number and the transverse flow parameter ϕ.

EQUIPMENT AND PROCEDURES

The experimental equipment is shown in Figure 3. The axial air stream is produced by a centrifugal blower. Before entering the porous test section, the air stream goes through a bell-mouth entrance section, which contains a honeycomb plate, a fiberglass pad and straightening vanes to aid development of the velocity profile, and then through a 30-ft. section where equilibrium pipe flow is approached.

The helium injection port is an L-shaped piece of thin-walled brass tubing, 0.30 cm. in I.D. and 0.48 cm. in O.D., positioned so that its center is on the center line of the calming section and its tip is at the front edge of the test section. This tube is small enough not to disturb the axial air flow to any appreciable degree but large enough to permit reliable concentration measurements downstream. The helium is injected at a velocity that matches the center line velocity of the air stream.

The test section consists of a porous ceramic pipe, 2 ft. long and 6.026 in. in I.D., surrounded by an 8-in. aluminum pipe fitted with coaxial flanges. To induce transverse flow, filtered air is injected into the porous pipe through 14 symmetrically placed injection ports. Velocity is measured by a stainless steel pitot tube consisting of a ⅛-in. I.D. impact tube, and a 0.029-in. I.D. static tube.

Gas samples are withdrawn from the impact tube by a vacuum pump at a rate close to isokinetic and, after circulating through a sampling valve and a 1-ft. coil of copper tubing, are analyzed on a chromatograph. Concentrations are determined from the height of the chromatographic peaks, which are very sharp. Reproducibility is about 3%, and readings down to about 0.01% can be taken with a good degree of confidence. Although concentrations as low as 0.001 are detectable, reproducibility is poor at such low levels.

As a basis for determining fluid properties, temperatures are measured by thermocouples connected to a potentiometer pyrometer. A more detailed description of the equipment is given in (*16*) and (*21*).

Experiments were run at Reynolds numbers from 12,000 to 66,000, corresponding to average velocities between 4.36 and 23.0 ft./sec., with air injection velocities ranging from 0 to 0.170 ft./sec. The highest injection rate ($\phi = -0.0362$) corresponded to injection of 58% by volume of the main stream. The values of ϕ, (v_w/u_{avo}), the dimensionless blowing parameter, used were 0, −0.00792, −0.01572, −0.0362, and

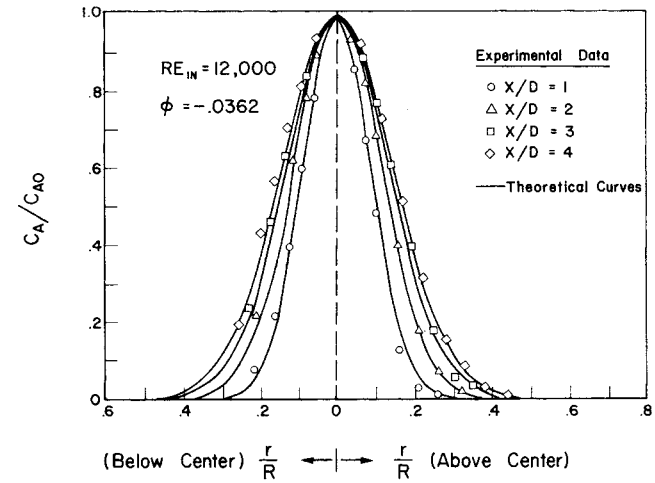

Fig. 4. Comparison of theoretically predicted conc. profiles with experimental data with fluid injection at the wall.

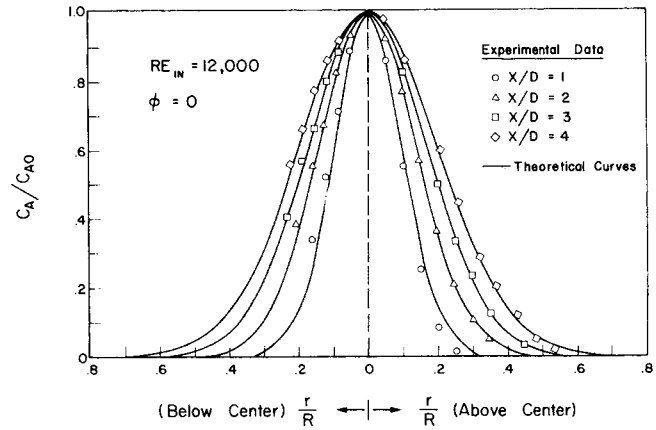

Fig. 5. Comparison of theoretically predicted conc. profiles with experimental data with no transverse flow.

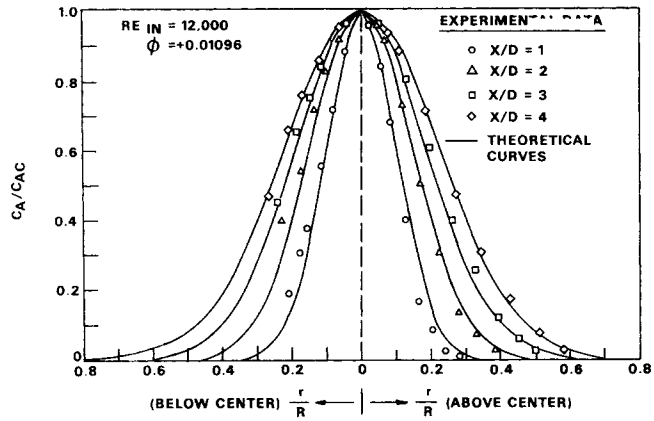

Fig. 6. Comparison of theoretically predicted conc. profiles with experimental data with fluid suction at the wall.

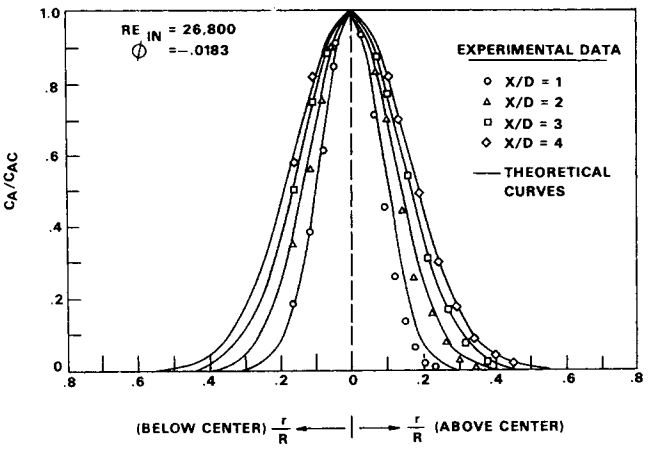

Fig. 7. Comparison of theoretically predicted conc. profiles with experimental data with fluid injection at the wall.

+0.01096 for Re_{IN} = 12,000; 0, −0.00417, −0.0183 and +0.00389 for Re_{IN} = 26,800; 0, +00.00263 for Re_{IN} = 49,400; and 0 and −0.00575 for Re_{IN} = 66,000.

Velocity profiles were taken before the concentration profiles so that the discharge rate from the injection tube could be calculated. Each reading required a waiting time of between 15 and 45 min. for the manometer to come to equilibrium. Velocity traverses were taken only to about 1.8 in. from the pipe center. For the concentration profiles, several samples were analyzed at each radial position and the results were averaged. For the first sample at each position, the waiting period ranged from about 1 min. for a high Reynolds number to about 5 min. for a low Reynolds number. This procedure ensured that the first sample reflected the actual concentration at the point in question and not a mixture of the new sample with part of the previous sample. For all samples after the first, the waiting period ranged from ¾ to 3 min., depending on the Reynolds number.

RESULTS AND DISCUSSION

Typical dimensionless concentration profiles at various values of the aspect ratio (x/D) and of the injection or suction parameter (ϕ) are shown in Figures 4 through 7, where the solid lines are the theoretical curves calculated from Equation (15) and the points are experimental data. Comparison for relatively high values of ϕ only is shown since it represents a rather severe test of the theory. As may be seen from these figures, the theoretical curves agree closely with the data at all values of x/D except the smallest, that is, 1.0. This discrepancy may be partially due to the disturbances introduced by the injection tube. The experimentally determined concentration profiles were somewhat skewed at x/D = 1.0, which confirms previous observations for the case of no transverse flow (7). They were centered by plotting the data and taking the center corresponding to the maximum concentration.

These curves display the strong effect of transverse flow on the concentration profiles of the tracer. For example, the dimensionless concentration (C_A/C_{AC}) at aspect ratio of 3 and r/R of 0.2 is 0.52 in the absence of transverse flow but is only 0.32 for an injection parameter of −0.0362 and is about 0.57 for suction parameter equal to +0.01096. It is also shown later in this paper (see Figure 8) that

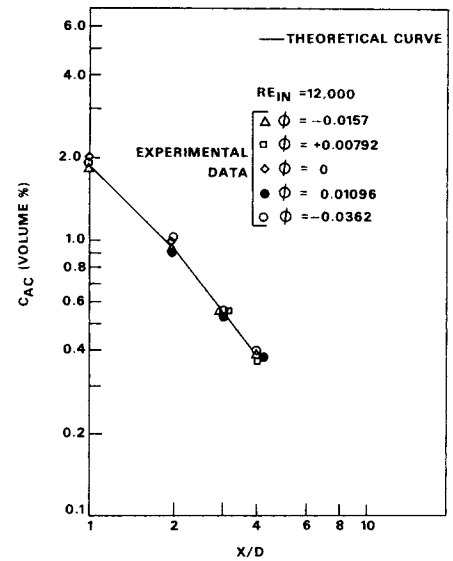

Fig. 8. Comparison of predicted C_{Ao} with experimental values.

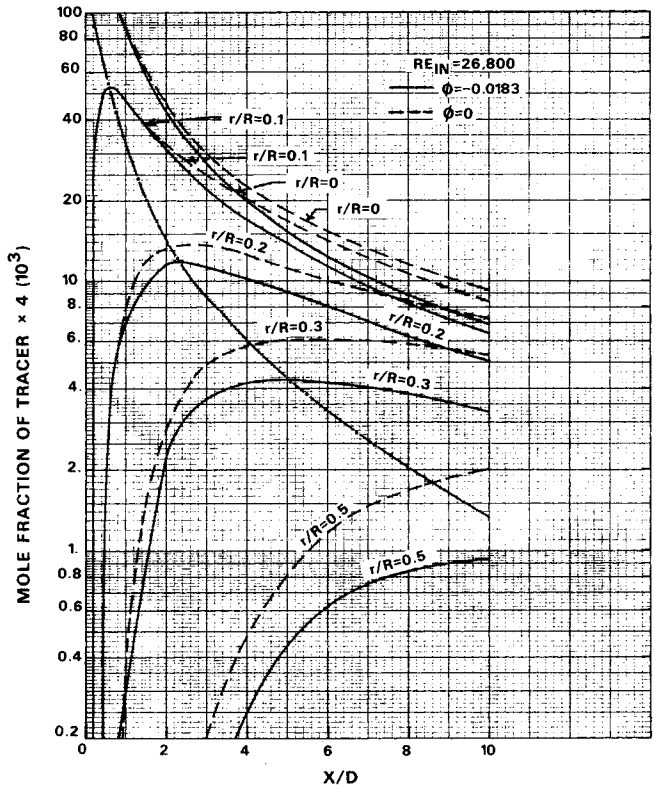

Fig. 9. Theoretically calculated C_A versus aspect ratio for fluid injection at the wall.

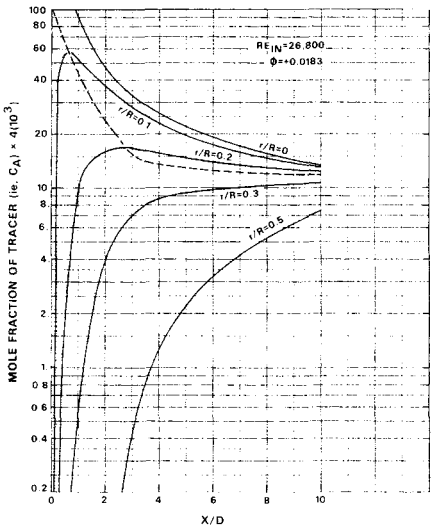

Fig. 10. Theoretically calculated C_A versus aspect ratio for fluid suction at the wall.

the concentration at the pipe axis (C_{AC}) is hardly affected by transverse flow. This means that the dilution effect of injection (due to the inerts added) predominates over its so called squeezing effect (due to the inward radial velocity) whereas for suction through the pipe walls, the dispersing effect (due to the outward radial velocity) is less important than its concentrating effect (due to the withdrawal of inerts). This suggests the possibility of using transverse injection as a method for achieving dynamic dilution and preventing the wall corrosion due to the corrosive compounds in the carrier gas inducted flows.

The Figures 4 through 7 also show how the plume width of the dispersing material is affected by transverse flow. For instance, as shown in Figure 4, for Re_{IN} = 12,000, $\phi = -0.0362$, and $x/D = 4$, the width of the plume is only about 46% of the radius. By contrast, as shown in Figure 6, for Re_{IN} = 12,000, $\phi = +0.01096$, and $x/D = 4$, the plume width is about 77% of the radius. Thus, material removed radially through the walls tends to spread the dispersing material away from the pipe axis, while the injected material tends to squeeze the dispersing material toward the axis. These effects further increase with increase in the suction and injection rates at any given value of Re_{IN}.

Figure 8 compares the experimentally determined concentrations of the dispersing material at the pipe axis with those calculated from Equation (16) for Re_{IN} = 12,000 and various values of x/D and ϕ. Again, the agreement is satisfactory. It is interesting to note from this figure that the concentration at the pipe axis is hardly affected by the transverse flow, thereby implying that the effect of transverse flow has not yet penetrated down to the pipe axis. This is to be expected for a short tube such as used in our experiments.

The tracer mole fraction values calculated from Equations (15) and (16) are plotted versus x/D in Figures 9 and 10 for Re_{IN} = 26,800. For an r/R less than b/R, the tracer concentration is maximum at the injection tube (that is, $x/D = 0$) and decreases monotonically as x/D increases. By contrast, for a radial distance more than the injection tube radius from the pipe axis, the tracer concentration is zero at $x/D = 0$ and goes through a maximum at some value of x/D. This value increases as the radial distance from the pipe axis increases. The loci of these maxima are shown by broken lines in these figures. Apparently, injection through the pipe walls makes this locus steeper by bringing about the concentration maximum earlier than in the absence of transverse flow, while suction makes it flatter.

The ratio of core eddy diffusivities for material transport in the presence and absence of transverse flow, as calculated from Equation (19), is plotted versus x/D in Figure 11. This ratio increases with injection and decreases with suction. Moreover, with an increase in x/D, this ratio increases for injection and decreases for suction. The increase in eddy diffusivity due to injection can be used to achieve better mixing in reactors such as the secondary combustion chamber of a furnace, etc.

Figure 12 displays the ratio of radial mass fluxes in the presence and absence of fluid injection versus the dimensionless radial distance from the pipe axis for a Re_{IN} = 26,800 and various values of x/D. The results show that the radial flux enhancement factor $[N_{Ar}/(N_{Ar})\ \phi = 0]$ is

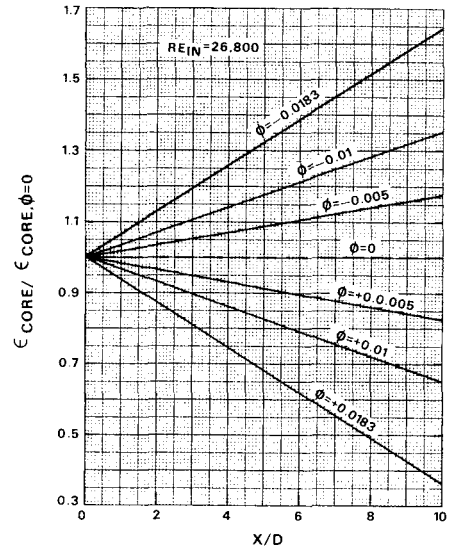

Fig. 11. Calculated enhancement factor for core eddy diffusivity versus aspect ratio.

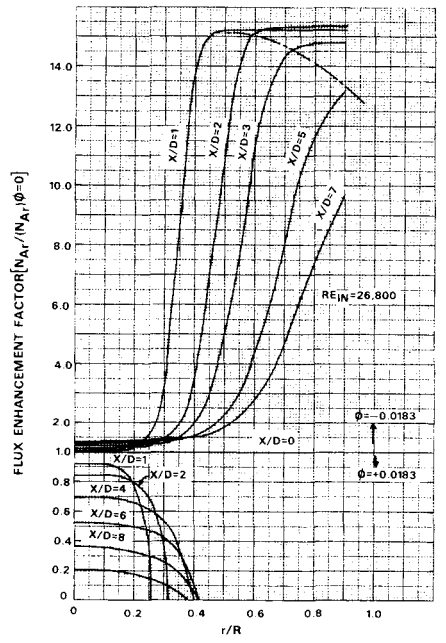

Fig. 12. Predicted enhancement factor for radial mass flux of tracer versus radial distance from pipe axis.

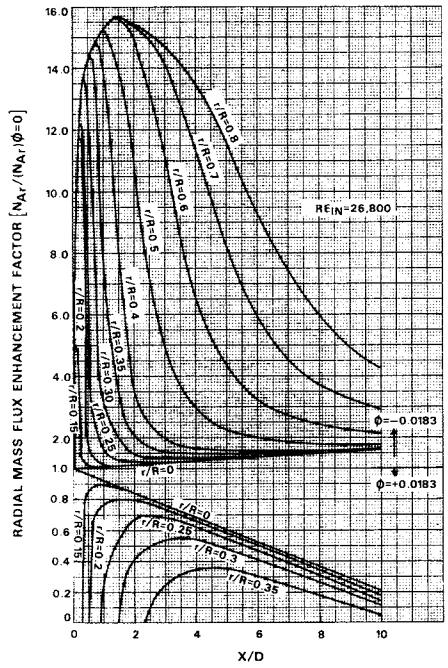

Fig. 13. Predicted enhancement factor for radial mass flux of tracer versus aspect ratio.

larger than 1.0 in the presence of injection and less than 1.0 in the presence of suction.

Figure 12 also shows that in the presence of injection, at a particular value of x/D, the enhancement factor first remains constant with an increase in the dimensionless radial distance from the pipe axis, then starts increasing, and finally reaches a constant value. The locus of the points at which the enhancement factor reaches a constant asymptotic value is shown by a broken line. Just the opposite occurs with suction. Here, at a particular value of x/D, the enhancement factor first remains constant with an increase in the dimensionless radial distance from the pipe axis, then starts decreasing until it reaches zero value.

Finally, Figure 13 displays the radial mass flux enhancement factor versus x/D for $Re_{IN} = 26{,}800$ and various values of the dimensionless radial distance from the pipe axis. In the presence of injection, at a particular value of r/R, the enhancement factor first increases with increase in x/D, goes through a maximum and then starts decreasing. For suction also, except near the pipe axis, the enhancement factor first increases with increase in x/D, goes through a maximum and then starts decreasing.

CONCLUSIONS

The following conclusions can be drawn from the present study:

1. Analytical expression presented here [Equation (15)] can be used to calculate the concentration of a gaseous tracer at any radial and downstream location in the pipe core with uniform fluid injection or suction. The values predicted by this equation are in good agreement with the experimental data.

2. The width of the plume of the dispersing tracer is considerably affected by transverse flow. Equation (15) can be used to predict the plume width fairly accurately.

3. The tracer concentration at the pipe axis varies with longitudinal distance and the transverse flow parameter. These variations can be calculated by using Equation (16). The values predicted by this equation agree fairly well with the experimental values (see Figure 8).

4. The present analysis shows that the eddy diffusivity for material transport in the central core of the pipe increases with injection and decreases with suction through the pipe walls. Also for increasing values of aspect ratio, the eddy diffusivity decreases in the case of suction and increases in the case of injection.

5. The mass flux in the radial direction increases with fluid injection and decreases with fluid suction.

ACKNOWLEDGMENT

The authors gratefully acknowledge the financial assistance provided by the Fine Particle Section of I.I.T. Research Institute. The assistance provided by Amoco Chemicals Corporation in the preparation of this manuscript is greatly appreciated.

NOTATION

b = inside radius of the injection tube
C_A = concentration of the gaseous tracer
C_{Ac} = concentration of the gaseous tracer at the pipe axis
D = diameter of the porous pipe
D_{AB} = molecular diffusivity of gaseous tracer
u^* = dimensionless longitudinal velocity, $= u/u_{av}$
N_{Ar} = mass flux of tracer in the radial direction
Q = volumetric injection rate of tracer. For isokinetic injection, this is $\pi b^2 u_{c0}$
R = pipe radius
u, v = longitudinal and radial velocities of fluid respectively
u_{c0} = velocity at the pipe axis for the case of no transverse flow
u_c = velocity at the pipe axis
u_{av} = average velocity in the longitudinal direction
v = radial velocity
v_w = radial velocity at the pipe wall
x, r = longitudinal and radial coordinates

Greek Letters

ϵ = eddy diffusivity for material transport
ϵ_{c0} = eddy diffusivity at the pipe axis for the case of no injection or suction
ϕ = transverse flow parameter $(= v_w/u_{av0})$. This is negative for injection and positive for suction

Subscripts

c = refers to the pipe axis
0 = refers to the absence of transverse flow
i = refers to the inlet condition

LITERATURE CITED

1. Baldwin, L. V., and T. J. Walsh, *AIChE J.*, **7**, 53 (1961).
2. Baldwin, L. V., and W. R. Michelsen, *J. Engr. Mech. Div., Am. Soc. Civil Eng.*, **88**, 37 (1962).
3. Bernard, R. A., and R. H. Wilhelm, *Chem. Eng. Prog.*, **46**, 233 (1950).
4. Becker, H. A., R. E. Rosenweig, and J. R. Gwozdz, *AIChE J.*, **12**, 964 (1966).
5. Boothroyd, R. G., *Trans. Inst. Chem. Engrs.*, **45**, 1297 (1967).
6. Flint, D. L., Ph.D., thesis, Univ. Illinois, Urbana (1958).
7. ———., H. Kada, and T. J. Hanratty, *AIChE J.*, **6**, 325 (1960).
8. Friedlander, S. K. and H. F. Johnstone, *Ind. Eng. Chem.*, **49**, 1151 (1957).

9. Frenkiel, F. N., "Advances in Applied Mechanics," Vol. 3, Academic Press, New York (1953).
10. Hanratty, T. J., G. Latinen, and R. H. Wilhelm, *AIChE J.*, **2**, 372 (1956).
11. Hinze, J. O., "Turbulence," McGraw-Hill, New York (1959).
12. Kalinske, A. A., and C. L. Pien, *Ind. Eng. Chem.*, **36**, 220 (1944).
13. Lee, J., and R. S. Brodkey, *AIChE J.*, **10**, 186 (1964).
14. Mickelsen, W. R., *NACA Tech. Note 3570* (1955).
15. McCarter, R. J., L. F. Stutzman, and H. A. Koch, *Ind. Eng. Chem.*, **6**, 41 (1949).
16. Randhava, S. S., M.S. thesis, Ill. Inst. Tech., Chicago (1966).
17. Schlinger, W. G., and B. N. Sage, *Ind. Eng. Chem.*, **45**, 657 (1953).
18. Sherwood, T. K., and B. B. Woertz, *Trans. Am. Inst. Chem. Engr.*, **35**, 517 (1939).
19. Schubauer, G. B., *NACA Tech. Rept.*, 524 (1935).
20. Soo, S. L., H. E. Ehring, and A. F. Kouh, *Trans. ASME, Series D*, **82**, 609 (1966).
21. Suneja, S. K., Ph.D. thesis, Ill. Inst. Tech., Chicago (1970).
22. Sutton, O. G., *Proc. Roy. Soc. (London), A135*, 143 (1932).
23. Sutton, O. G., *Proc. Roy. Soc., (London), A146*, 701 (1934).
24. Taylor, G. I., *Proc. London Math Soc.*, **20**, 196 (1921).
25. Taylor, G. I., *Proc. Roy. Soc. (London), 151A*, 421 (1935).
26. Towle, W. L., and T. K. Sherwood, *Ind. Eng. Chem.*, **31**, 457 (1939).
27. Groenhoe, M. C., *Chem. Eng. Sci.*, **25**, 1005 (1970).

Manuscript received November 24, 1970; revision returned July 20, 1971; paper accepted August 2, 1971.

Foam Separation of Complex Anions: Silver Thiosulfate

DIBAKAR BHATTACHARYYA and ROBERT B. GRIEVES

Department of Chemical Engineering
University of Kentucky, Lexington, Kentucky 40506

An experimental study is conducted of the ion flotation of $Ag(S_2O_3)^-$ and $Ag(S_2O_3)_2^{3-}$ from an aqueous solution at pH 4.5 with a cationic surfactant. For initial solutions 2.0×10^{-3} to 8.0×10^{-3} M in total silver, optimum silver flotation at foam cessation is achieved at a molar thiosulfate to silver ratio (Th/Ag) of 0.75 and surfactant to silver ratio (EHDA/Ag) of 0.5, at Th/Ag = 1.0 and EHDA/Ag = 1.1, and at Th/Ag = 2.0 and EHDA/Ag = 2.2. The silver flotation is 99^+, 98^+, and 92^+ % at the three sets of ratios, respectively. At Th/Ag > 2.0, highly efficient flotation cannot be achieved due to decreased particle size, and perhaps by competition with free $S_2O_3^{2-}$ for the surfactant.

The stoichiometry of the ion flotation product is established from relative silver and surfactant flotation rates. The stoichiometry is independent of foaming time, but is a strong linear function of EHDA/Ag and Th/Ag, in contrast to the stoichiometry of flotation products of other simple and complex anions. Rate data can be fit reasonably by a first-order reversible model. The rate constant is an inverse function of EHDA/Ag, indicating the desirability of pulsed surfactant addition. Results are discussed in terms of the average ligand number of silver, particle size, and surface potential measurements.

Ion flotation is a foam separation process which involves the formation in aqueous solution of an insoluble product between an ionic surface-active agent and an ion (colligend) of charge opposite to that of the long-chain surfactant ion. The product may be formed in the bulk solution or only at higher concentrations which result from the accumulation of the surfactant at the surface layers of gas bubbles dispersed through the solution (*1* to 3). The particulate product is collected by the bubbles and is carried into a foam or froth rising above the bulk solution. A

Correspondence concerning this paper should be addressed to R. B. Grieves.